Korean J. Chem. Eng., 39(7), 1688-1708 (2022)
DOI: 10.1007/s11814-022-1098-z

pISSN: 0256-1115
eISSN: 1975-7220

A combined cycle power plant integrated with a desalination system: Energy, exergy, economic and environmental (4E) analysis and multi-objective optimization

Behrad Haghghi, Amin Saleh, Hassan Hajabdollahi, and Mohammad Shafiey Dehaj†

Department of Mechanical Engineering, Faculty of Engineering, Vali-e-Asr University of Rafsanjan, Rafsanjan, Iran
(*Received 14 November 2021 • Revised 27 February 2022 • Accepted 2 March 2022*)

Abstract−A cogeneration production system of power and freshwater was studied from the perspective of energy, exergy, economic, and environmental (4E). The main components of this system include a Brayton cycle (BC), dual-pressure heat recovery steam generator (HRSG), steam turbine (ST), and multi-effect evaporation with thermal vapor compression (MEE-TVC). The system was optimized with a multi-objective genetic algorithm using MATLAB software and by considering the performance of two objective functions: the total annual cost (TAC) to minimize and the thermal efficiency to maximize. The results showed that, with increasing gas turbine inlet temperature, thermal efficiency, exergy efficiency, and emission of pollutants improved, but the gain output ratio (GOR) decreased. GOR of desalination system, exergy efficiency of combined cycle power plant (CCPP), and emission of pollutants improved by increasing the compressor pressure ratio. In investigating the number of effects in desalination unit, by increasing this parameter the production of freshwater, GOR and exergy efficiency of MEE-TVC was increased. By adding a duct burner to the cogeneration system, the thermal efficiency, the exergy efficiency, and the net power output were reduced by 0.67, 3.9, and 5.91%, respectively. But the freshwater production, GOR, and TAC was improved about 7.97, 9.69, and 1.265%, respectively.

Keywords: Cogeneration Production of Power and Freshwater; Multi-effect Evaporation with Thermal Vapor Compression (MEE-TVC), HRSG, Total Annual Cost (TAC), Exergy Efficiency

INTRODUCTION

Energy consumption in many countries is one of the important factors of economic development. But energy efficiency is more important than energy consumption because it affects how the country grows economically [1]. The most basic energy sources in the world today are fossil fuels. These resources have a limited lifespan and have a significant impact on environmental pollution [2]. Since in the current situation it is not possible to use other sources completely instead of fossil fuels, it is necessary to consider how to use them and effective strategies to increase their productivity [3,4], because it promotes economic development and reduces environmental pollution [5,6]. Also, life, health, and continuous development are constantly dependent on freshwater. In the world, the water consumption of domestic, industrial and agricultural is 10, 20 and 70% of the total amount of water consumption, respectively. About 97% of the planet's waters are salty and the rest are fresh [7].

One of the most important applied technologies is the use of systems for the cogeneration production of power and water (CPW), especially in areas facing shortages of freshwater resources, such as the Persian Gulf [8,9]. Therefore, different methods for desalination of seawater have been studied by researchers. Thermal methods of seawater desalination are generally in the category: multi-stage flash (MSF) and multi-effect evaporation with thermal vapor compression (MEE-TVC) [10,11]. In the MEE-TVC system, due to the low operating pressure of the effects, the water temperature rises to about 70 °C. So, the system is a good case to use the extra heat of the systems [12,13].

According to the previous literatures, combined and cogeneration systems were examined from different perspectives. For example, Esmaieli et al. optimized the power generation system by genetic algorithm to achieve the best system layout [14]. The combined cycle power plant was investigated from a thermo-economic perspective by Petrovic [15] and Mohammadi [16] by a multi-objective genetic algorithm. The prime mover of the studied systems is the gas cycle, and the exhaust heat of the gas turbine is recovered by HRSG and given to the Rankin cycle. The exergo-economic optimization of gas turbines with absorption chillers was investigated using an evolutionary algorithm by Ahmadi et al. [17]. Mohtaram [18] and Yazdi [19] studied the combined cycle power plant from an economic perspective using an evolutionary algorithm, respectively, with the objective functions of reducing pollutant emissions - increasing exergy efficiency and reducing the total annual cost - increasing exergy efficiency. A mathematical model for the MEE-TVC of a steady-state was developed by Mutaz [20] and compared with commercial systems. Salimi et al. [21,22] optimized the MEE by recovering the heat of the internal combustion engine and by using this system in the steam cycle. Their results showed that with increasing the number of effects, the GOR of desalination increased. In the analysis of energy and exergy of the multi-effect distillation desalination system by Guo et al. [23], the results showed that by increasing the temperature difference between the effects and the temperature of the motive steam of the first effect, the GOR and

†To whom correspondence should be addressed.
E-mail: m.shafiey@vru.ac.ir

exergy efficiency increased. Due to the high heat loss in the gas cycle, its combination with the system makes sense. In one research, Ahmadi et al. [24] examined this hybrid system. The results showed that the total annual cost increases with increasing compressor pressure ratio and the number of effects. In another research, Alzahrani et al. [25] analyzed the performance of the simultaneous power and water production system with the main drive of the gas turbine. The results demonstrated that by increasing the pressure ratio of the gas turbine, the amount of produced water flow is slightly reduced, and the exergy efficiency of the cogeneration plant is increased.

As discussed in the above paragraph, modeling of combined cycle power plant with desalination unit from the perspective of energy and exergy has been sufficiently investigated. But, the effect of desalination design parameters, the effect of duct burner and environmental impacts on cogeneration system performance were not investigated as well. According to the previous works, several researchers have proposed a combined system of power and water production. However, there are few researches reporting the progress of cogeneration systems. On other hand, a multi-effect evaporation with thermal vapor compression (MEE-TVC) unit can operate either single or in combination with other systems. Therefore, due to the need for further research, the present study examines the system of simultaneous production of power and freshwater. Main components include a Brayton cycle (BC), a dual-pressure heat recovery steam generator (HRSG), a steam turbine (ST), and MEE-TVC unit. The proposed system is optimized from a thermo-economic point of view and examined from an energy, exergy, economic and environmental (4E) perspective. Finally, the advantage of the purpose system compared to the Brayton cycle is expressed. In brief, here are the contributions of this study:

- Modeling and 4E analysis were expressed of combined cycle power plants using Multi-effect evaporation with thermal vapor compression (CCPPW).
- Brayton cycle is considered as the main mover of the system.
- In the proposed system, waste heat from Brayton cycle serves as a source of heat to produce power and desalinated water.
- Modeling and optimization of the system is developed with MATLAB software and leads to minimum total annual cost (TAC) and to maximum thermal efficiency of the system by multi-objective genetic algorithm (NSGA-II). Also, the thermodynamic properties of different parts of the system are extracted from engineering equation solving software (EES).
- System performance with and without duct burner is investigated.
- Finally, the results are presented and the influence of design parameters on system performance was investigated.

SYSTEM MODELING

A combined CCPPW system including a Brayton cycle (BC), a Rankine cycle (RC), a dual-pressure heat recovery steam generator (HRSG), multi-effect evaporation with thermal vapor compression (MEE-TVC) is illustrated in Fig. 1. The air enters the compressor at the atmospheric condition and leaves this compressor with high pressure and high temperature. The air temperature of the compressor outlet in the air preheater increases. The compressed air enters the combustion chamber (CC) where it reacts with the injected fuel, which is pure methane in the present study, and its temperature rises considerably. Then, hot gases enter the gas turbine and produce useful work. To the couple, a desalination unit with a Brayton cycle, extra equipment is required. Since the primary energy of MEE-TVC is steam, this extra equipment should have the ability to produce motive steam. This is done through an HRSG. Turbine outlet gases thus enter this component, and their energy is recovered. High-pressure steam is used to produce power to the steam turbine, and low-pressure steam is used to produce the driving steam into the desalination system.

1. Assumptions of Power Generation System

The combinations of energy and mass balance equations are numerically solved and the temperature and enthalpy of each line of the system are predicted. The assumptions of the power generation system are as follows:

- All the processes are steady-state and steady flow.
- The fuel injected to the combustion chamber is assumed to be pure methane.
- The principle of ideal-gas mixture is applied for the combustion products.
- The total pressure drop of the gas side in the heat recovery steam generator is 5% [26].
- The dead-state conditions are P_0=1.013 bar and T_0=298.15 K.
- Heat loss from the combustion chamber is considered to be 3% of the fuel lower heating value [24]. Moreover, all other components are considered adiabatic.
- Combustion chamber pressure drop is 5%. Also, pressure drop in air preheater of air and gas flow side is 5% and 3%, respectively [26].
- The process of evaporators is constant temperature and only the steam quality increases.
- The deaerator evaporator is in an ideal condition, namely, its pressure is constant.
- The pressure of the steam condenser is constant and its value is 0.09 bar.
- The output of the economizer is saturated liquid.
- The quality of the inlet and outlet steam side in the superheater is 100% and, in this equipment, only the steam temperature increases.

2. Energy Analysis

To model the system, the first law of thermodynamics is applied for the following sub-sections. To simulate the system, the thermophysical properties of working fluids are obtained from engineering equation solving software, and the optimization algorithm is NSGA-II developed by MATLAB software.

2-1. Brayton Cycle

The Brayton cycle, which is the main prime mover of this CCPPW system, has a significant role in power generation. Also, the Brayton cycle waste heat can be recovered in the HRSG to produce high and low-pressure steams.

- Air compressor

$$T_B = T_A \times \left(1 + \frac{1}{\eta_{is,Ac}}\left(Rp_{Ac}^{\frac{\gamma_a - 1}{\gamma_a}} + 1\right)\right) \quad (1)$$

In Eq. (1) $\eta_{is,Ac}$ is the isentropic efficiency of air compressor, Rp_{Ac}

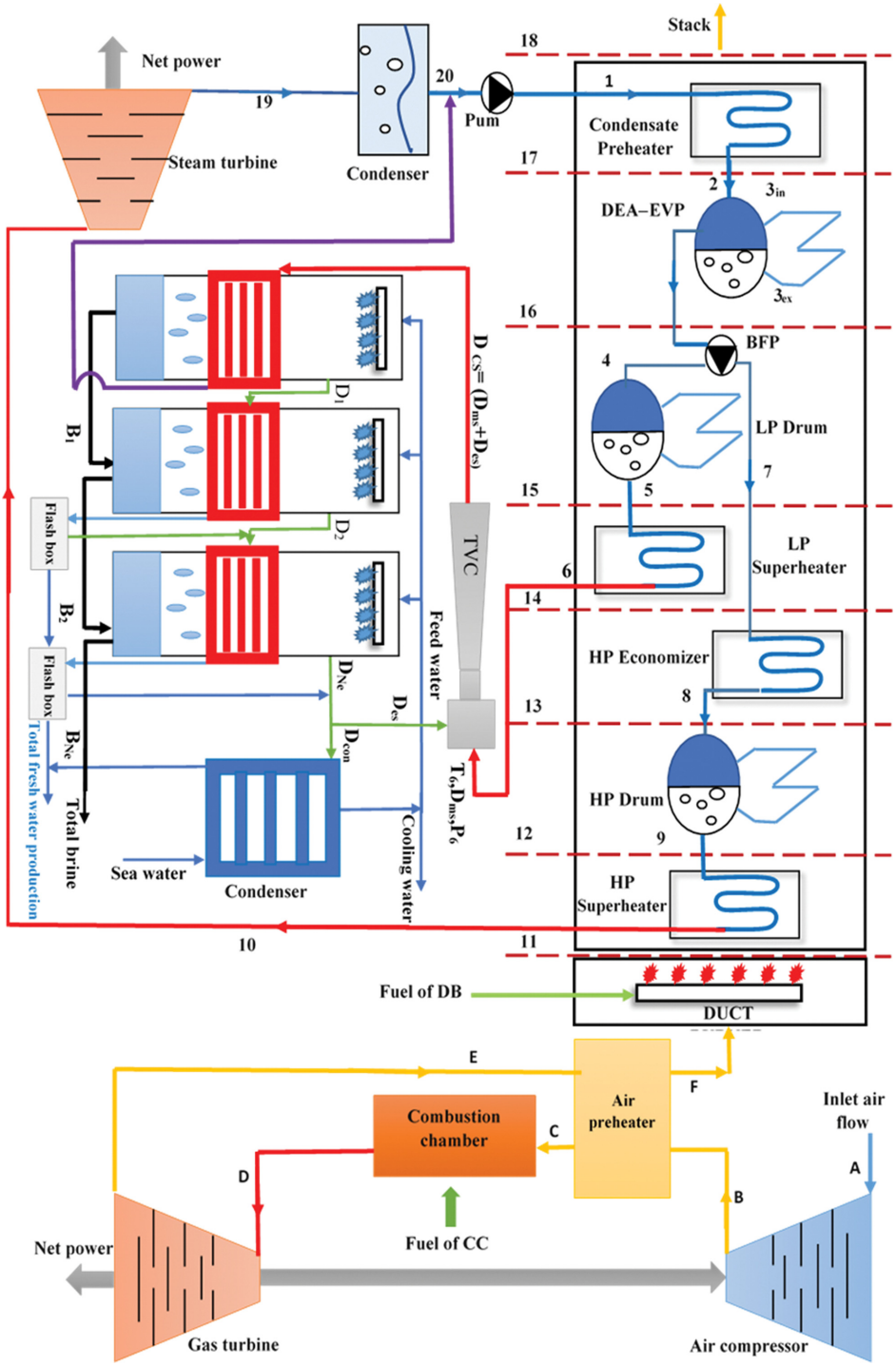

Fig. 1. Schematic of the proposed integrated system.

is the air compressor pressure ratio and γ_a is the air specific heat ratio [24]. Also, according to the compressor pressure ratio, the pressure of point B is obtained from the following equation:

$$\frac{P_B}{P_A} = Rp_{Ac} \tag{2}$$

$$\dot{W}_{Ac} = \dot{m}_a C_{pa}(T_B - T_A) \tag{3}$$

where $\dot{m}_a$ is the air mass flow rate and is constant pressure specific heat of air, which is considered as a function of temperature [24,26].

- Air preheater

The energy balance equation for air preheater is obtained from the following equation [24,26]:

$$\dot{m}_a(h_C - h_B) = \dot{m}_g(h_E - h_F)\eta_{Aph} \tag{4}$$

$$\frac{P_C}{P_B}=(1-\Delta P_{Aph}) \tag{5}$$

where ΔP_{Aph} is the pressure drop along the regenerator and η_{Aph}= 0.81 is the regenerator effectiveness [24].

- Combustion chamber

In combustion analysis, the air is treated as a combination of O_2 and N_2. Thus, other gases (water vapor and CO_2) are neglected, and dry air is approximated as 21% of O_2 and 79% of N_2. The combustion reaction concerning pure methane fuel is expressed as follows [27]. At high temperatures, nitrogen oxide (NO_x) is produced, which is very important in environmental analysis.

$$CH_4+2O_2+N_2\rightarrow CO_2+2H_2O+N_2+NO_x+CO+\text{heat} \tag{6}$$

The energy balance of the combustion chamber is obtained as follows [26]:

$$\dot{m}_a h_C+\dot{m}_f \text{LHV}=\dot{m}_g h_D+(1-\eta_{cc})\dot{m}_f \text{LHV} \tag{7}$$

$$\frac{P_D}{P_C}=(1-\Delta P_{cc}) \tag{8}$$

Here, LHV=50,000 (kJ/kg) for the lower heating value of pure methane fuel, η_{cc}=0.98, ΔP_{cc}, efficiency and combustion chamber pressure drop, respectively [24,26].

- Gas turbine

$$T_E=T_D\left\{1-\eta_{is,\,GT}\left[1-\left(\frac{P_D}{P_E}\right)^{\frac{1-\gamma_g}{\gamma_g}}\right]\right\} \tag{9}$$

$$\dot{W}_{GT}=\dot{m}_g C_{pg}(T_D-T_E) \tag{10}$$

In Eq. (10) C_{pg} is the specific heat capacity, which is considered as a function of temperature and $\dot{m}_g$ is the mass flow rate of the gas stream, which is expressed as the sum of air and fuel inlet [26]:

$$\dot{m}_g=\dot{m}_a+\dot{m}_f \tag{11}$$

2-2. Rankine Cycle

- Heat recovery steam generator

HRSG produces steam at high and low-pressure levels. High-pressure steam is given to the Rankine cycle to generate power. Two pinch points temperature (i.e., temperature difference between the evaporator output gas (T_{13} and T_{16}) and the saturation state ($T_{st,\,LP}$ and $T_{st,\,HP}$)) can be defined in a dual-pressure HRSG. According to the first law of thermodynamics, the energy balance for equipment is expressed as follows [28]:

- Duct burner

$$\dot{m}_g h_F+\dot{m}_{f,\,DB}\text{LHV}=(\dot{m}_g+\dot{m}_{f,\,DB})h_{11}+(1-\eta_{DB})\dot{m}_{f,\,DB}\text{LHV} \tag{12}$$

In Eq. 12, h, $\dot{m}_{f,\,DB}$, η_{DB}=0.93 are gas stream enthalpy, mass flow rate of fuel and efficiency of duct burner, respectively [29,30]. In general, the energy balance for other components of the HRSG is expressed as follows [24,25]:

$$\dot{m}_g C_{pg}(T_{in}-T_{out})=\dot{m}_s(h_{out}-h_{in}) \tag{13}$$

- Steam turbine

$$\dot{m}_{s,\,HP}(h_{10}-h_{19})=\dot{W}_{ST} \tag{14}$$

$$\eta_{ST}=\frac{\dot{W}_{ST,\,ac}}{\dot{W}_{ST,\,is}} \tag{15}$$

- Condenser

$$\dot{Q}_{cond}=\dot{m}_{s,\,HP}(h_{10}-h_{19}) \tag{16}$$

- Feed water pump

$$\dot{W}_{fwp}=\dot{m}_w(h_{19}-h_{20}) \tag{17}$$

$$\eta_{fwp}=\frac{\dot{W}_{fwp,\,ac}}{\dot{W}_{fwp,\,is}} \tag{18}$$

where η_{fwp} are $\dot{W}_{fwp,\,is}$ pump isentropic efficiency and isentropic work.

2-3. Multi-effect Evaporation with Thermal Vapor Compression

MEE-TVC is one of the most effective desalination methods. This system has an essential role in the production of freshwater in many regions of the world, especially in the Persian Gulf countries. An MEE-TVC system includes few evaporators and flash boxes, a condenser, a steam ejector. The performance of the ejector is such that the compressive energy of the steam entering the ejector in the convergent part is converted into kinetic energy, and due to the reduction of the cross-sectional area the steam velocity increases to supersonic. After passing through the fixed diameter part (throat), it enters the divergent part (diffuser) and its pressure increases. The steam output of the ejector enters the first effect of the MEE-TVC by passing between the pressure of the motive steam and the suction steam. Then in the first effect, the feed water is sprayed on the evaporating pipes and part of it evaporates and the other part enters the next effect as brine, which has a higher concentration than the feed water. The steam produced in effect 1 enters effect 2 as a motive steam and this action is repeated in all steps. From effect 2 to the last effect, there is a flash box. Condensed steam in effect 2 enters the flash box of the same effect and due to its lower working pressure compared to the effect, part of it evaporates and enters effect 3 with motive steam produced by effect 2, and this process continues until the last effect. The feed water after entering the condenser due to heat exchange with the output steam of the last effect, the output steam becomes liquid and the temperature of the feed water increases. Part of the feed water returns to the sea and the other part enters each effect in parallel. Fig. 2(a) shows a schematic of MEE-TVC.

Modeling assumptions and equations governing the MEE-TVC unit are as follows:

- All the processes are steady-state and steady flow.
- The steam produced in each effect is considered salt-free.
- The boiling point elevation (BPE=0.8) is equal for all effects [20,24].
- According to environmental conditions, the maximum percentage of brine concentration of the last effect is 70,000 ppm [20,24].
- The system is considered sediment-free.
- Thermodynamic losses are negligible.
- The temperature difference between all the effects is constant and is obtained from the following equation [20,21,24]:

$$\Delta T=\frac{T_{B1}-T_{B,\,Ne}}{Ne-1} \tag{19}$$

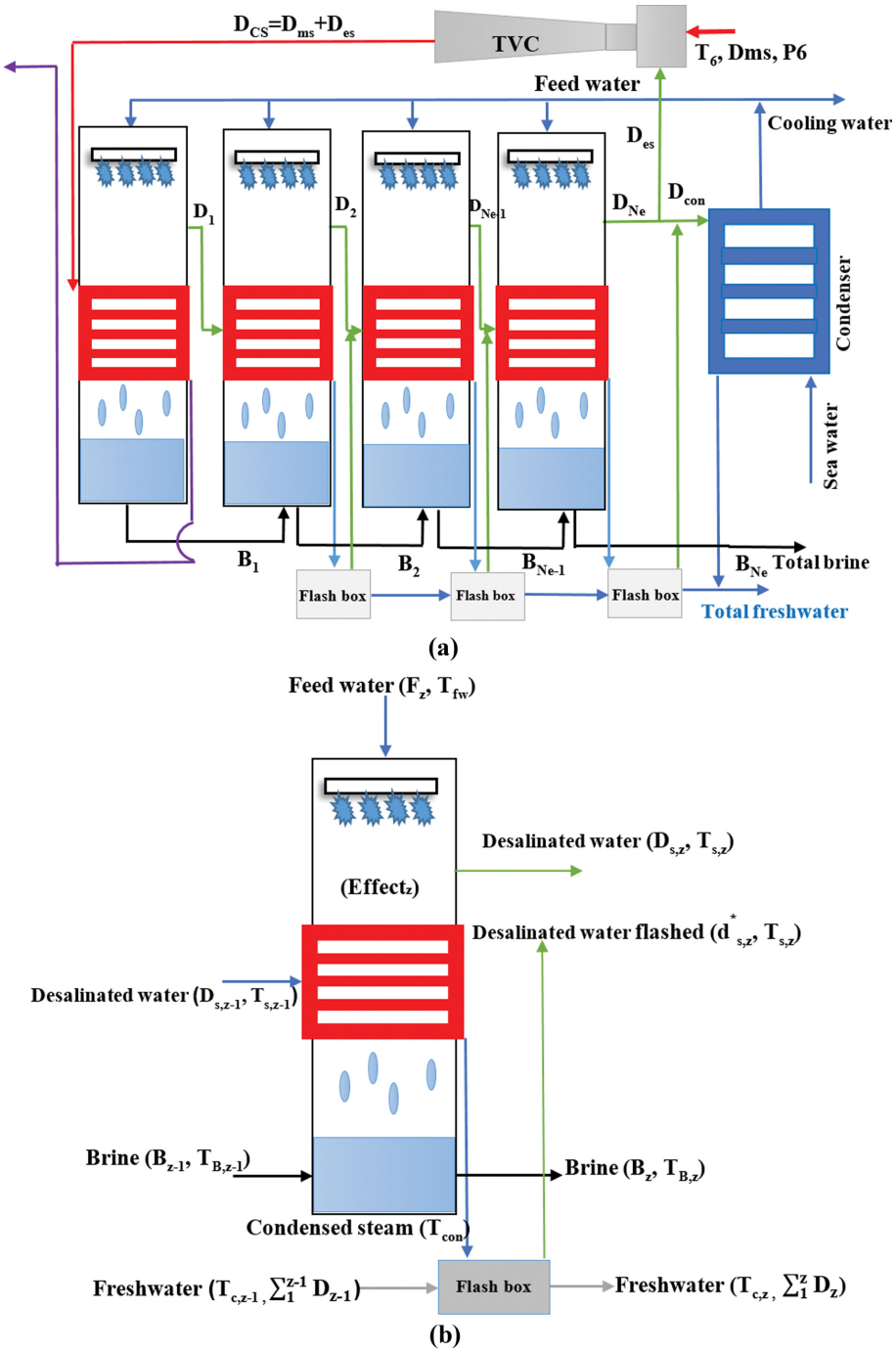

Fig. 2. (a) Shows a schematic of MEE-TVC and (b) Shows a schematic of the energy and mass balance in each z-effect.

where T_{B1}, $T_{B,Ne}$ and Ne are the top brine temperature of first effect, top brine temperature of last effect and number of effects, respectively. Fig. 2(b) shows the mass and energy balance in each effect of the MEE-TVC system. The mass and energy balance for the MEE-TVC system is given in Appendix-A in Table A1.

According to the top brine temperature in each effect and the temperature difference between the effects, the top brine temperature in the next effect is obtained the following relation [20,24]:

$$T_{B,z+1}=T_{B,z}-\Delta T \qquad z=1, 2, 3, \ldots, Ne \tag{20}$$

The boiling point elevation in each effect and the specific heat capacity of water, taking into account the salt concentration (X_B) and its temperature ($T_{B,Ne}$), follow Eqs. (21) and (22), respectively [20,24]:

$$bpe=X_B(a+(b\times X_B))/1{,}000 \tag{21}$$

$$C_p=[a_1+(a_2T_{B,Ne})+(a_3(T_{B,Ne})^2)+(a_4(T_{B,Ne})^3)]/1{,}000 \tag{22}$$

In Eq. (22) the temperature is in °C and the water salinity is in g/kg. a and b are constant [20,24].

In the ejector, there are three important parameters: entrainment ratio (ER), expansion ratio (Er), and compression ratio (CR), which have a good effect on its performance and are obtained the following relationships, respectively [20,31]:

$$ER = 0.235\frac{(P_{cs})^{1.19}}{(P_{es})^{1.04}} \times (Er)^{0.015} \quad (23)$$

$$Er = \frac{P_{ms}}{P_{es}} \quad (24)$$

$$CR = \frac{P_{cs}}{P_{es}} \quad (25)$$

According to the motive steam of first effect and the entrainment ratio, the amount of entrained steam is obtained [20,24]:

$$D_{es} = \frac{D_{cs}}{ER} \quad (26)$$

The steam temperature in each effect is also obtained from the relation [20]:

$$T_{s,z} = T_{B,z} - bpe \qquad z = 1, 2, 3, \ldots, Ne \quad (27)$$

Given that the system is fed in parallel, the amount of feed water for each effect is obtained by dividing the total feed water by the number of effects [20,24]:

$$F_z = \frac{F}{Ne} \qquad z = 1, 2, 3, \ldots, Ne \quad (28)$$

The gain output ratio (GOR) of desalination is obtained according to the ratio of the total mass flow rate of the freshwater produced to the mass flow rate of the motive steam [20,24,32]:

$$GOR = \frac{D_{tot}}{D_{ms}} \quad (29)$$

3. Energy Performance

Using the first law of thermodynamics, the ratio of useful production work to input energy of CCPP is expressed as follows:

$$\eta_{th,\,CCPP} = \frac{\dot{W}_{net,\,GT} + \dot{W}_{net,\,ST} - \dot{W}_{pump}}{\dot{m}_f LHV} \quad (30)$$

Here, $\dot{m}_f$ is mass flow rate of fuel consumption ($\dot{m}_f = \dot{m}_{f,\,cc} + \dot{m}_{f,\,DB}$).

4. Exergy Analysis and Performance

Exergy consists of two important parts: chemical exergy and physical exergy. In this research, the kinetic and latent components of exergy are negligible. Exergy is defined as the maximum professional useful work that can be obtained as a system interacts with an equilibrium state. Therefore, the specific exergy of each flow can be calculated from the following equation [30]:

$$ex = ex_{ph} + ex_{ch} \quad (31)$$

where ex_{ph} is a physical exergy and is obtained from the following equation [30]:

$$ex_{ph} = (h - h_o) - T_o(s - s_o) \quad (32)$$

The mixture chemical exergy is obtained from the following equation [30,33]:

$$ex_{mix}^{ch} = \sum_z^n X_z ex_{ch} + \sum_z^n X_z \ln X_z \quad (33)$$

where X is the molar fraction of each element.

The physical exergy of streams of brine, and feed water, desalinated can be obtained as follows [24]:

$$\dot{E}x_{ph} = \dot{m}\left(C_p(T, X) \times (T - T_o) \times C_p(T - T_o) \times \log\left(\frac{T}{T_o}\right)\right) \quad (34)$$

The chemical exergy is obtained from the following equation [24]:

$$\dot{E}x_{ch} = \dot{m}(N_{mol}(X, M_w, M_s) \times 10^{-3} \times (8.314) \times T_o \times (-X_w - \log X_w - X_s \times \log X_s) \quad (35)$$

$$X_w = \frac{N_{pure}(X, M_w)}{N_{mol}(X, M_w, M_s)}$$

$$X_s = \frac{N_{salt}(X, M_s)}{N_{mol}(X, M_w, M_s)}$$

$$N_{pure} = \frac{1{,}000 - X}{M_w}$$

$$N_{salt} = \frac{X}{M_s}$$

$$N_{mol} = N_{pure} + N_{salt}$$

Here, N_{mol}, X_w, X_s, M_s=18 g, M_w=58.5 g are the number of particles, fraction of water, fraction of salt, molar weight of salt and molar weight of water, respectively [24].

The second law of thermodynamics, defined as the product exergy output divided by the input exergy, for the Brayton cycle, CCPPW and MEE-TVC, can be expressed as follows [23,24,33]:

$$\eta_{ex,\,BC} = \frac{\dot{W}_{net,\,GT}}{\dot{E}x_f} \quad (36)$$

$$\eta_{ex,\,MEE\text{-}TVC} = \frac{\dot{E}x_{D_{tot}} - \dot{E}x_{D_{con,\,in}}}{\dot{E}x_{D_{ms,\,in}} - \dot{E}x_{D_{cs,\,out}}} \quad (37)$$

$$\eta_{ex,\,CCPPW} = \frac{\dot{W}_{net,\,GT} + \dot{W}_{net,\,ST} + \dot{E}x_{D_{tot}} - \dot{E}x_{D_{con,\,in}}}{\dot{E}x_f} \quad (38)$$

where $\dot{E}x_f = \dot{m}_f LHV\xi$ is the fuel exergy. Also, the specific exergy loss (ξ) for pure methane is 1.06 [29].

5. Environmental Impact Evaluation

Environmental impact can be reduced by increasing efficiency, which leads to reduced fuel consumption. Given that there is much research in the field of energy and exergy, but little of it has addressed the issue of the environment. The present research focuses on the emission of CO_2, CO and NO_x in the combustion chamber as environmental pollutants. The fuel reaction and adiabatic flame temperature are two factors on which the emission of pollutants depends. Pollutant emissions can be calculated as follows [32,35,36]:

$$\dot{m}_{CO_2} = 44.01 \times X_{CO_2} \times (\dot{m}_f / M_f) \quad (39)$$

$$\dot{m}_{CO} = \frac{0.179E9\exp\left(\frac{7{,}800}{T_{pz}}\right)}{P_D^2 \tau \left(\frac{\Delta P_{in}}{P_{in}}\right)^{0.5}} \quad (40)$$

$$\dot{m}_{NO_x} = \frac{0.15E16\,\tau^{0.5}\exp\left(\frac{-71{,}100}{T_{pz}}\right)}{P_D^{0.05}\,\tau\left(\frac{\Delta P_{in}}{P_{in}}\right)^{0.5}} \quad (41)$$

where, x is the molar ratio of carbon in the fuel and M_f the molecular weight of the fuel. τ the residence time in the combustion zone (τ is assumed constant and is equal to 0.022 s [32]), P_C is the combustor inlet pressure, $\Delta P_{in}/P_{in}$ is the non-dimensional pressure drop in the combustion chamber, T_{pz} is the adiabatic flame temperature in the primary zone of the combustion chamber and is expressed by the following equation [37,38]:

$$T_{pz} = A\,\sigma^{\alpha}\exp(\beta(\sigma+\lambda)^2)\,\pi^x\,\theta^y\,\psi^z \quad (42)$$

Here π the dimensionless pressure P/P_o (P being the combustion pressure P_C), θ is a dimensionless temperature T/T_o (T being the inlet temperature T_C), ψ is the H/C atomic ratio (ψ=4, the fuel being pure methane [31]), ($\sigma=\phi$) ϕ being the fuel to air equivalence ratio (ϕ=0.68 is assumed constant [31]), x, y and z are quadric functions [32,33]. Also, A, α, β and λ are constants in these equations and their value is given in references [32,33]. In this study, the cost coefficient for CO_2, CO and NO_x is 0.02086 $/kg, 6.853 $/kg and 0.024 $/kg, respectively [24].

CASE STUDY AND MODEL VALIDATION

The proposed system is presented according to the environmen-

Table 1. Properties of the coastal site of Asaluyeh located in the south of Iran

Ambient temperature (°C) [40]	Seawater temperature (°C) [41,42]	Seawater Salinity (ppm) [43]
25	35	41,000

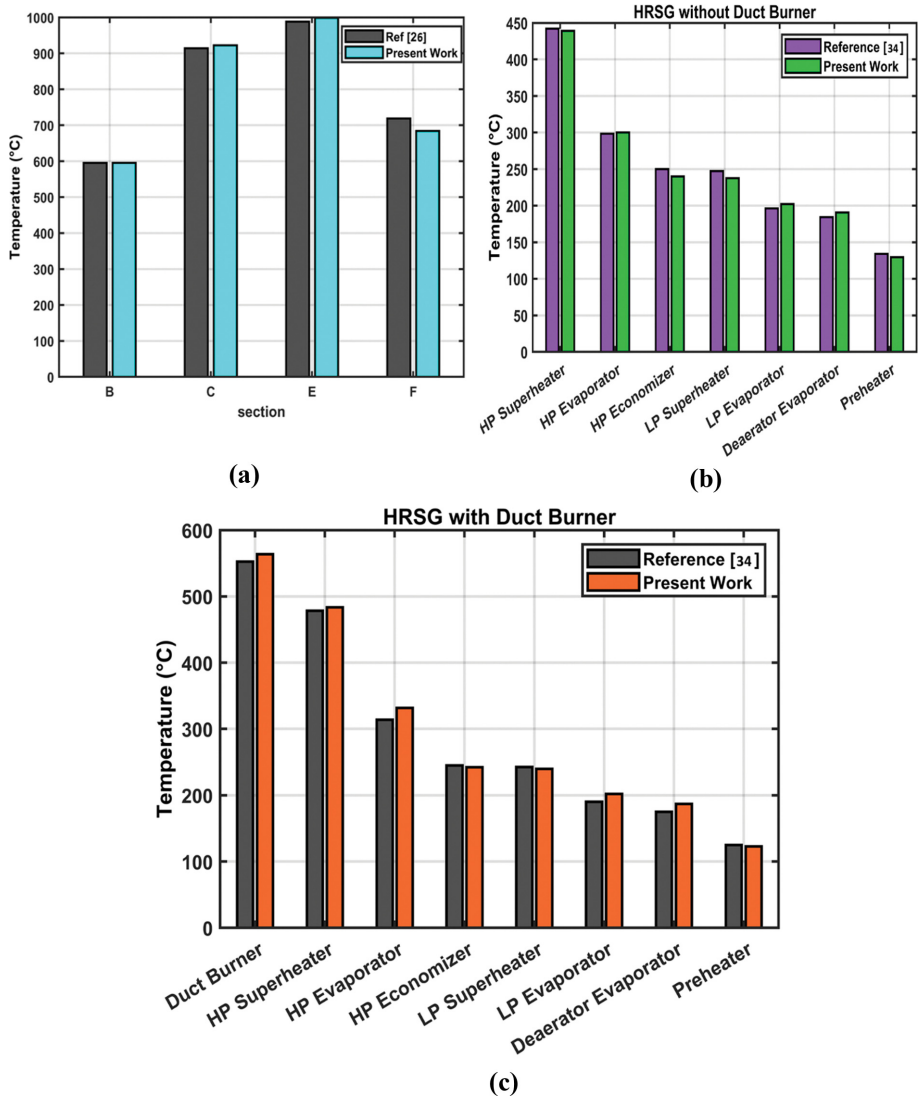

Fig. 3. (a) Variation of the gas temperature in parts of the Brayton cycle compared to reference [26], (b), (c) Variation of hot gas temperature at different parts of HRSG compared to reference [34].

Table 2. Brayton cycle performance parameters compared to reference [26]

Parameter	Model	Reference	Difference (%)
Mass flow rate of air (kg/s)	101.42	99.4559	1.97
Mass flow rate of fuel (kg/s)	1.6662	1.6274	2.39
Compressor work (kW)	30,855.6	29,692.2	3.92
Turbine work (kW)	60,855.4	59,692.5	1.95

Table 3. The output results in different parts of the MEE-TVC system to reference

System	Model	Ref. [20]	Difference (%)	Ref. [38]	Difference (%)
Design conditions					
Number of effects Ne	4	4	-----	4	-----
Motive pressure P_{ms}, kPa	2,300	2,300	-----	2,300	-----
Top brine temperature T_{B1}, °C	40.1	40.1	-----	40.1	-----
Minimum brine temperature T_{Ne}, °C	45.4	45.4	-----	45.4	-----
Temperature difference per effect, °C	4.9	4.9	-----	4.9	-----
Feed seawater temperature T_f, °C	41.5	41.5	-----	41.5	-----
Cooling seawater temperature T_{cw}, °C	31.5	31.5	-----	31.5	-----
Motive steam flow rate D_M, kg/s	8.8	8.8	-----	8.8	-----
TVC					
Entrainment ratio ER	1.14	1.14	-----	1.14	-----
Expansion ratio ER	240.9	240.9	-----		-----
Compression ratio CR	2.65	2.65	-----		-----
System performance					
Distillate production D, kg/s	58.2	58.02	0.3	57.8	0.6
Gain output ratio GOR	6.61	6.59	0.3	6.51	1.5
Specific heat consumption Q, kJ/kg	382.81	370.8	3.2	NA	-----
Specific heat transfer area Ad, m^2/kg/s	270.3	277.1	2.5	NA	-----

tal conditions of Asaluyeh city, which is in the south of Iran. Environmental and coastal conditions for Asaluyeh city are listed in Table 1.

- **Brayton cycle**

The calculation code for the Brayton cycle with air preheater has been developed in MATLAB software, and to determine the thermodynamic properties of the various parts of the cycle, MATLAB software has been linked to EES. To validate the modeling, the model output was compared with the same input data as the reference [26]. Note that there is an acceptable percentage difference between the output data due to changes in some hypotheses to develop and model the model. Fig. 3(a) shows the output data for temperature in parts of the cycle. The amount of turbine production work, compressor consumption work, mass flow rate of fuel consumption, and mass flow rate of air for the model and reference [26] are presented in Table 2. According to Table 2 the highest percentage difference in compressor equipment is observed at 3.92%.

- **HRSG**

To validate the heat recovery steam generator modeling, the temperature of the gas side in different parts is compared with the reference [34] and this order is done with the same input data. Also, Fig. 3(b), (c) shows the comparison of exhaust gas temperatures in different parts of the system, for the model and reference [34]. To compare HRSG with and without duct burner, the highest percentage difference is observed in high pressure level evaporator and high-pressure level economizer, respectively.

- **MEE-TVC**

System modeling was performed in MATLAB software and to validate the performance of the model, its output was compared with the same input data as scientific reference [20] and commercial reference [39], and the results can be Acceptance was obtained. Table 3 shows the output results in different parts of the MEE-TVC system relative to the references. The highest percentage of difference in specific heat consumption was observed at 3.2%.

ECONOMIC ANALYSIS

Economic analysis is an important step in any feasibility study for the functional evaluation of a project concerning financial implications. Economic analysis includes estimates of total investment cost, total annual cost, capital recovery coefficient, operating and maintenance coefficient, and some other economic variables that provide information about the total cost and benefits of investments. The main output of the economic analysis report is the estimation of the capital cost of the components and the cost of their opera-

tion and maintenance (depending on the desired size and performance) and the cost of fuel. Therefore, the total annual cost (TAC) is determined as follows [33]:

$$TAC(\$/year) = \dot{C}_f + CRF \times \varphi \times \dot{C}_{inv} + \dot{C}_{env} \quad (43)$$

Here, φ, CRF, $\dot{C}_f$, $\dot{C}_{inv}$, $\dot{C}_{env}$ are the operation and maintenance coefficient, the capital recovery factor, cost rate of fuel, investment cost of equipment, and cost of the effects of polluting gases on the environment, respectively, and are expressed as follows [32,36]:

$$CRF = z_{eff}\frac{(1+z_{eff})^y}{(1+z_{eff})^y} \quad (44)$$

$$\dot{C}_f = (C_f \dot{m}_f LHV) \times time \quad (45)$$

$$\dot{C}_{inv} = \sum_n \dot{C}_n \quad (46)$$

$$\dot{C}_{env} = C_{CO}\dot{m}_{CO} + C_{NO_x}\dot{m}_{NO_x} + C_{CO_2}\dot{m}_{CO_2} \quad (47)$$

where, z_{eff}, y are the effective annual interest rate and the operating years for which the system is expected to operate (system lifetime). Also, time is the operating hours of the system in one year and $\dot{C}_n$ is the investment cost of each component of the system. The investment cost performance of each equipment and some parameters in the economic relations of 43-46 are given in Tables B1 and B2 in Appendix B, respectively.

OBJECTIVE FUNCTIONS, CONSTRAINTS, AND DESIGN PARAMETERS

In the analysis of energy systems, especially cogeneration systems, system efficiency, and system costs are of great importance. In this research, is investigated the thermodynamic and thermo-economic analysis of the combined cycle using a multi-effect evaporation with thermal vapor compression. The system is optimized by a multi-objective genetic algorithm and the objective functions lead to the maximum combined-cycle thermal efficiency and the minimum total annual cost (TAC). The collection of 16 design parameters is considered, which shown in Table 4.

Constraints on the system in terms of structural and environmental conditions are as follows:

$3\,^{\circ}C < T_{pp} > 60\,^{\circ}C$

$T_{18} > 120\,^{\circ}C$

$X_z < 70{,}000$ ppm

$\dot{W}_{net,\,tot} \leq 200{,}000$ kW

$D_{tot} \geq 6{,}000$ m^3/day

$T_F > T_B$

$T_E > T_C$

Also, the exergy efficiency for the equipment is as follows:

$$\psi_z = \frac{\dot{E}x_p}{\dot{E}x_f} < 1$$

Table 4. Design parameters and their range

Design parameters	Range	Unit
Gas turbine inlet temperature	900-1,300	°C
Isentropic efficiency of air compressor	80-90	%
Compressor pressure ratio	6-15	-----
Isentropic efficiency of gas turbine	80-90	%
Steam high pressure	40-100	bar
Steam low pressure	3-40	bar
Mass flow ratio of steam	0.7-0.9	%
Isentropic efficiency of steam turbine	80-90	%
Terminal temperature difference of Superheater	15-50	°C
Mass flow rate of fuel in duct burner	0.2-1	kg/s
Top brine temperature	60-70	°C
Minimum brine temperature	40-50	°C
Feed seawater mass flow rate	100-500	kg/s
Feed seawater temperature	35-45	°C
Number of effects	3-12	-----
Cooling seawater temperature	25-35	°C

RESULTS AND DISCUSSION

In this paper, the proposed system of cogeneration production of power and freshwater was examined from the perspective of energy, exergy, economic and environmental. To determine the thermodynamic properties of working fluids, the code of the system simulated with MATLAB software was linked to EES software. The parametric analysis and evaluation of the system performance was done by variation of the design parameters. This was done according to the optimal point, the variation of one parameter, and keeping the other parameters constant. For exergy analysis the mole fraction of the inlet air was considered according to the reference (H_2O=0.019, CO_2=0.0003, O_2=0.2059 and N_2=0.7748) [25,27]. The total net power output of the power plant was 200 MW, and the amount of freshwater production was 6,000 m^3/day. Also, the fuel used in the power plant was pure methane.

Fig. 4 shows the Pareto optimal front for multi-objective optimization of CCPPW. Any point on this front represents a potential solution. According to the Pareto optimal front, the minimum

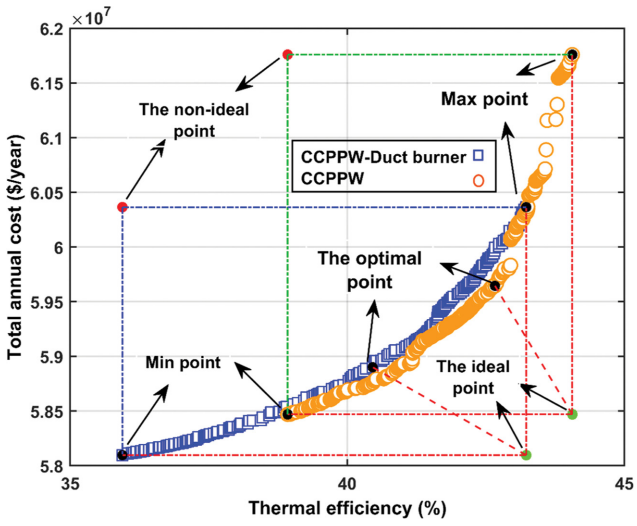

Fig. 4. The Pareto optimal front of proposed system.

Table 5. Optimized values of the design parameters of CCPPW- Duct burner

Optimal design parameters	Optimal point	Max point	Min point	Unit
Gas turbine inlet temperature	1,509.5	1,528.6	1,503.2	k
Compressor pressure ratio	13.3530	14.7001	11.8083	----
Isentropic efficiency of air compressor	84.96	84.88	83.62	%
Isentropic efficiency of gas turbine	87.48	88.03	86.38	%
HP steam pressure	58.1004	94.3670	40.8717	bar
LP steam pressure	4.8674	5.0691	5.3763	bar
Mass flow ratio of steam	89.92	88.59	88.35	%
Isentropic efficiency of steam turbine	88.19	90	80.16	%
Mass flow rate of fuel in duct burner	0.2945	0.2063	0.2126	kg/s
Terminal temperature difference of Superheater	35.9589	39.3135	25.5479	°C
Top brine temperature	67.3216	60.3715	60.5963	°C
Minimum brine temperature	43.6364	41.3392	40.1271	°C
Feed seawater temperature	43.6119	44.4135	43.7586	°C
Cooling seawater temperature	33.6901	30.6207	31.3586	°C
Feed seawater mass flow rate	404.7619	417.4603	201.5873	kg/s
Number of effects	7	5	5	----
System performance				
Net power output	192.990	196.370	184.580	MW
Thermal efficiency	40.4584	43.2283	35.7962	%
Exergy efficiency	39.2104	41.8652	34.2892	%
Fuel mass flow rate	8.1332	9.2450	10.5217	kg/s
HP pinch point temperature difference	5.0352	4.0622	26.5897	°C
LP pinch point temperature difference	35.2527	39.3212	40.4657	°C
Gain output ratio	13.4904	10.4180	10.2820	----
Distillated water	87.9950	76.9201	76.5133	kg/s
Pollutant of NO_x	0.0717	0.0721	0.1156	kg/s
Pollutant of CO	0.6107	0.5148	0.9494	kg/s
Pollutant of CO_2	1.2561	1.4278	1.6250	kg/s
Total annual cost	5.8900×10^7	6.0364×10^7	5.8097×10^7	$/year

point has the lowest thermal efficiency and total annual cost (TAC). It also can be seen that the maximum point has the highest thermal efficiency and TAC. The ideal point is defined as the point that has the highest thermal efficiency and the lowest TAC. The point that has the shortest distance to the ideal point is called the optimal point or suggested point. Also, the point with the highest cost and lowest thermal efficiency is called the non-ideal point. Fig. 4 shows that adding a duct burner to the system reduces the system's thermal efficiency and TAC. Tables 5 and 6 show the optimal parameters of systems with and without duct burner, respectively. According to the optimal point, with the addition of duct burner to the total power system, the thermal efficiency and exergy efficiency are reduced by 0.67, 3.9 and 5.9%, respectively. This is due to the approach of the power generation cycle to the steam cycle. From another perspective, with the addition of duct burner to the system, the temperature of combustion products increases, and thus the temperature of the recovered steam increases at different levels, especially the low-pressure level of the heat recovery steam generator. As a result, the freshwater production and GOR of desalination system are increased by 7.97 and 9.7%, respectively. With the addition of a duct burner to the system, the value of pollutant emissions increases about 11.41%, and the total annual cost decreases about 1.265%.

The total exergy efficiency of the CCPPW and the CCPPW-DB was calculated to be 41.5277 and 39.2104, respectively. According to Fig. 5(a), the CC has the highest exergy destruction rate. This is due to the irreversibility of combustion and the high-temperature difference between the flame temperature and the inlet air to the CC, which makes more entropy production. The second highest exergy destruction rate was observed in the HRSG, which is due to the temperature difference between the combustion gases and the steam at both high and low-pressure levels. The least exergy destruction rate was for the air preheater and the effects of water desalination unit. Due to low entropy production, less exergy destruction occurs in these levels. Fig. 5(b) shows the exergy efficiency in each part of the system, the most related to the air preheater and the least to the desalination system ejector. The reason for the low exergy efficiency in the ejector was due to the high difference in pressure and temperature of the primary and secondary flow as well as the compression ratio of the ejector.

In addition, the performance of the proposed system from a thermal point of view in the Brayton cycle improved about 25%. This

Table 6. Optimized values of the design parameters of CCPPW

Optimal design parameters	Optimal point	Max point	Min point	Unit
Gas turbine inlet temperature	1,515.9	1,547.6	1,503.2	k
Compressor pressure ratio	14.9028	14.9247	13.0042	----
Isentropic efficiency of air compressor	84.33	83.39	83.70	%
Isentropic efficiency of gas turbine	88.11	87.80	86.93	%
HP steam pressure	58.7706	76.4791	40.0305	bar
LP steam pressure	7.7074	7.7797	7.8339	bar
Mass flow ratio of steam	89.76	89.76	90	%
Isentropic efficiency of steam turbine	90	89.76	86.85	%
Terminal temperature difference of Superheater	36.3699	35	16.7808	°C
Top brine temperature	68.3675	65.7078	67.3118	°C
Minimum brine temperature	48.8270	47.5269	49.6090	°C
Feed seawater temperature	41.5787	41.8328	36.5054	°C
Cooling seawater temperature	30.5718	26.9550	29.8974	°C
Feed seawater mass flow rate	436.5079	411.1111	296.8254	kg/s
Number of effects	8	7	8	----
System performance				
Net power output	194.280	198.170	190.330	MW
Thermal efficiency	42.0340	44.0601	38.9229	%
Exergy efficiency	41.5277	42.6370	37.0965	%
Fuel mass flow rate	8.0518	9.4124	10.3650	kg/s
HP pinch point temperature difference	5.5553	3.1609	12.4757	°C
LP pinch point temperature difference	25.4107	27.8181	25.9553	°C
Gain output ratio	12.2990	11.4554	11.3909	----
Distillated water	81.4970	75.9073	73.7103	kg/s
Pollutant of NO_x	0.0547	0.0854	0.0954	kg/s
Pollutant of CO	0.4417	0.5329	0.7820	kg/s
Pollutant of CO_2	1.2436	1.4537	1.6008	kg/s
Total annual cost	5.9645×10^7	6.1759×10^7	5.8470×10^7	$/year

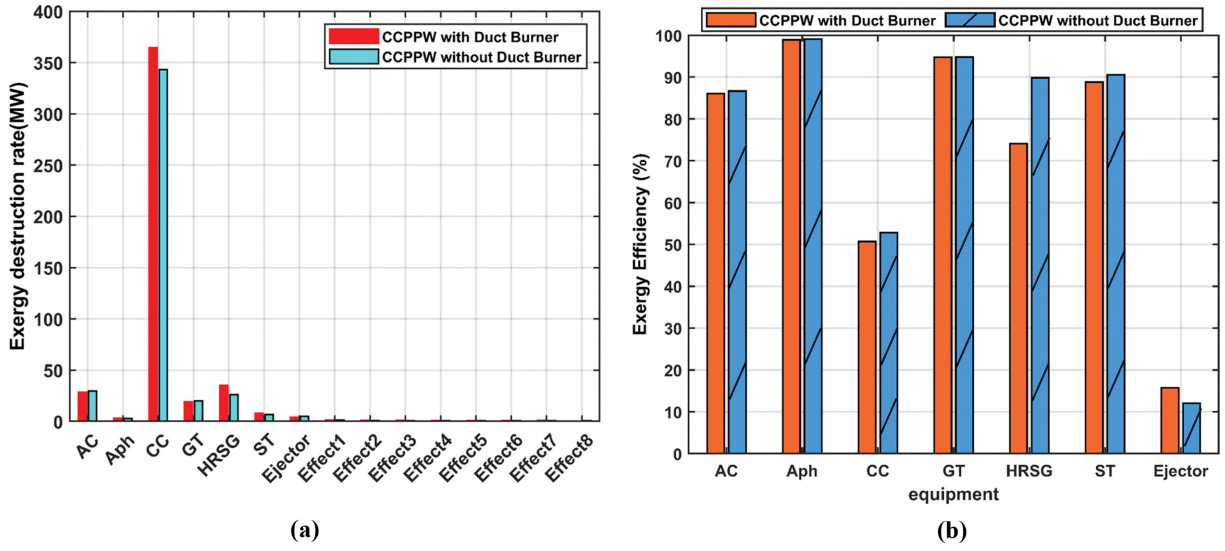

(a) (b)

Fig. 5. (a) Exergy destruction rate for each section of the system, (b) Exergy efficiency for each section of the system.

is due to the heat recovery of the hot exhaust gases of the gas turbine in the steam cycle. On other hand, in the combined cycle power plants, the thermal efficiency is about 45 to 50%. But, in the present study, due to the addition of a desalination unit in the low-pres-

sure level, the steam mass flow rate of the inlet to the ST is reduced. As a result, the production capacity of ST decreases, and the thermal efficiency of the current combined cycle is less than 45%.

1. Parametric Study

Some parameters have significant effects on the cogeneration system performance. Therefore, to determine the performance of the system with the operation parameters of system a parametric study was carried. The results are offered in several subsections.

- **Influence of gas turbine inlet temperature**

One of the most important parameters affecting the performance of the cogeneration system is the gas turbine inlet temperature (TIT). Fig. 6 shows the effect of gas turbine inlet temperature on system performance. Fig. 6(a) shows the effect of TIT on the thermal efficiency of the system in the Pareto optimal front. With increasing TIT, thermal efficiency increases. On other hand, the ratio of the power produced to the input energy increases. Also, Fig. 6(b) shows that as the inlet temperature of the gas turbine increases, the fuel mass flow rate of the CC and the mass flow rate of emission of pollutants decrease. This is due to the increase in gas turbine exhaust gas temperature and the increase in heat transfer in the air preheater, which increase the combustion chamber inlet air temperature by 25%. Sensitivity analysis of the TIT to affect the performance of MEE-TVC in Fig. 6(c) shows that as it increases, the mass flow rate of combustion products decreases. As a result, steam is recovered at a lower temperature at the low-pressure level of the HRSG. Since the flow of this level is given to the desalination system as a motive steam, the temperature of the motive steam of the first effect and the steam produced by this effect and other effects are reduced and as a result GOR of the desalination system is reduced. Fig. 6(d) shows that with increasing TIT, the exergy destruction rate decreases; however, due to the constant net power output, the fuel mass flow rate decreases and increases the exergy

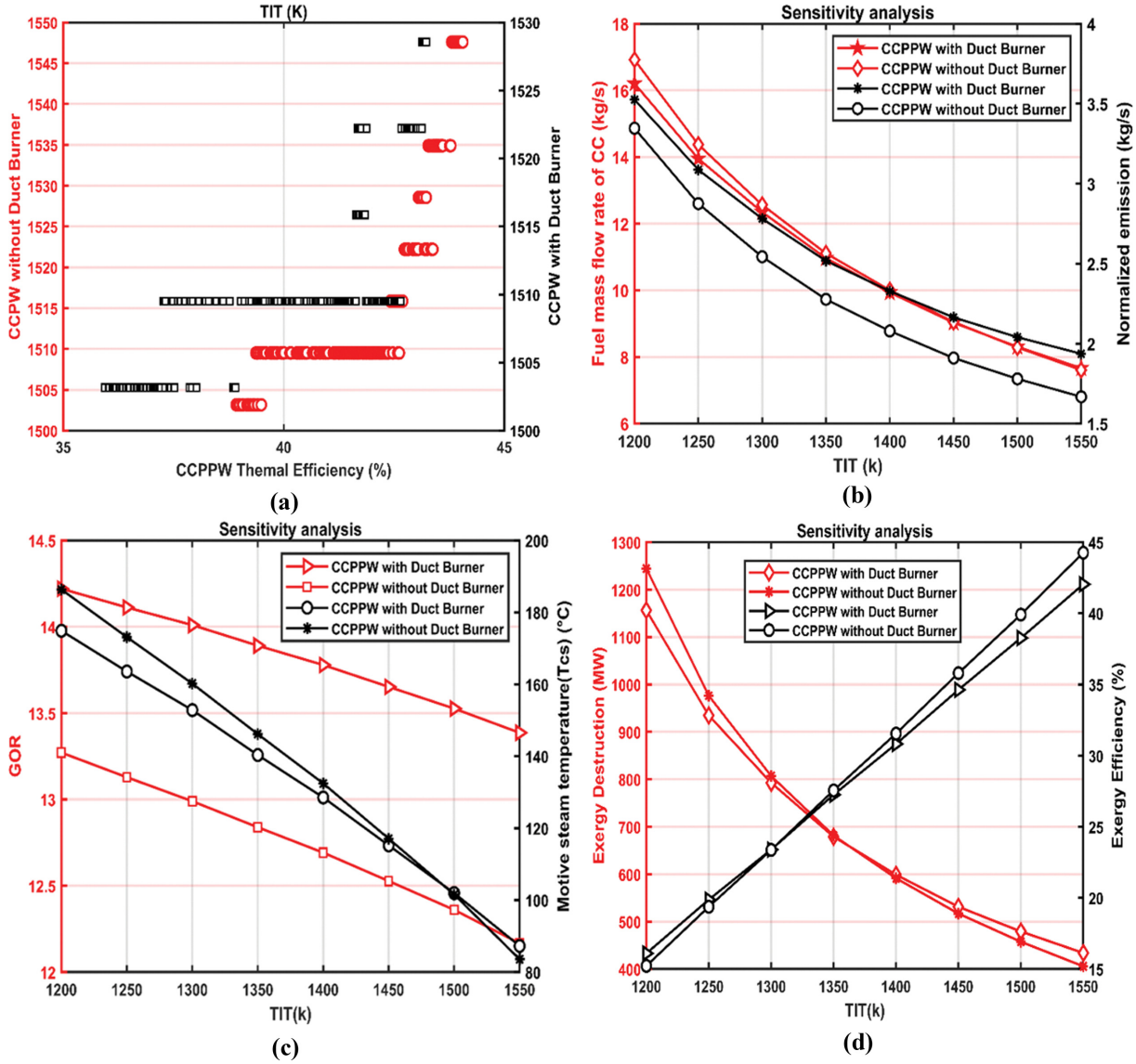

Fig. 6. (a) Effect of Gas TIT on system efficiency in Pareto optimal front, (b) Variation of fuel mass flow rate and normalized emission rate, (c) GOR and Motive steam temperature, (d) exergy destruction rate and exergy efficiency.

efficiency of the system. Finally, with the increase of the TIT, the total annual cost is reduced by about 52%, which is mainly due to the reduction of fuel consumption cost and investment cost of system equipment.

- **Influence of air compressor pressure ratio**

The air compressor is one of the most important pieces of equipment in the combined cycle. Therefore, considering the efficiency of the first law of thermodynamics, the variation of the performance parameters of system according to the air compressor pressure ratio (Rp_{Ac}) are illustrated in Fig. 7. According to Fig. 7(a), the thermal efficiency of the system increases with increasing compressor pressure ratio. According to Fig. 7(b) and increasing the compressor pressure ratio and other parameters are constant, especially the gas turbine inlet temperature and net power outlet, Therefore, the inlet air temperature to the combustion chamber increases. Due to this, the fuel inlet to the combustion chamber and the amount of emission pollutants are reduced and, as a result, the thermal efficiency of the system increases. However, at high efficiencies, this parameter decreases slightly as it increases compressor work and slightly increases fuel consumption. Also, Fig. 7(c) shows with increasing compressor pressure ratio, the temperature of the products of combustion increases about 24% and causes, increases in the temperature of the motive steam of the first effect and the GOR of the MEE-TVC. According to Fig. 7(d) with increasing Rp_{Ac}, fuel consumption is reduced by 8% and that causes exergy efficiency and exergy destruction rate in the system to increase and decrease, respectively. Finally, with the increase in this parameter, the total annual cost decreases by about 23%.

- **Influence of HRSG working pressure on high pressure level (HP)**

HRSG plays an important role in increasing the efficiency of the combined cycle. So, several design parameters are effective for de-

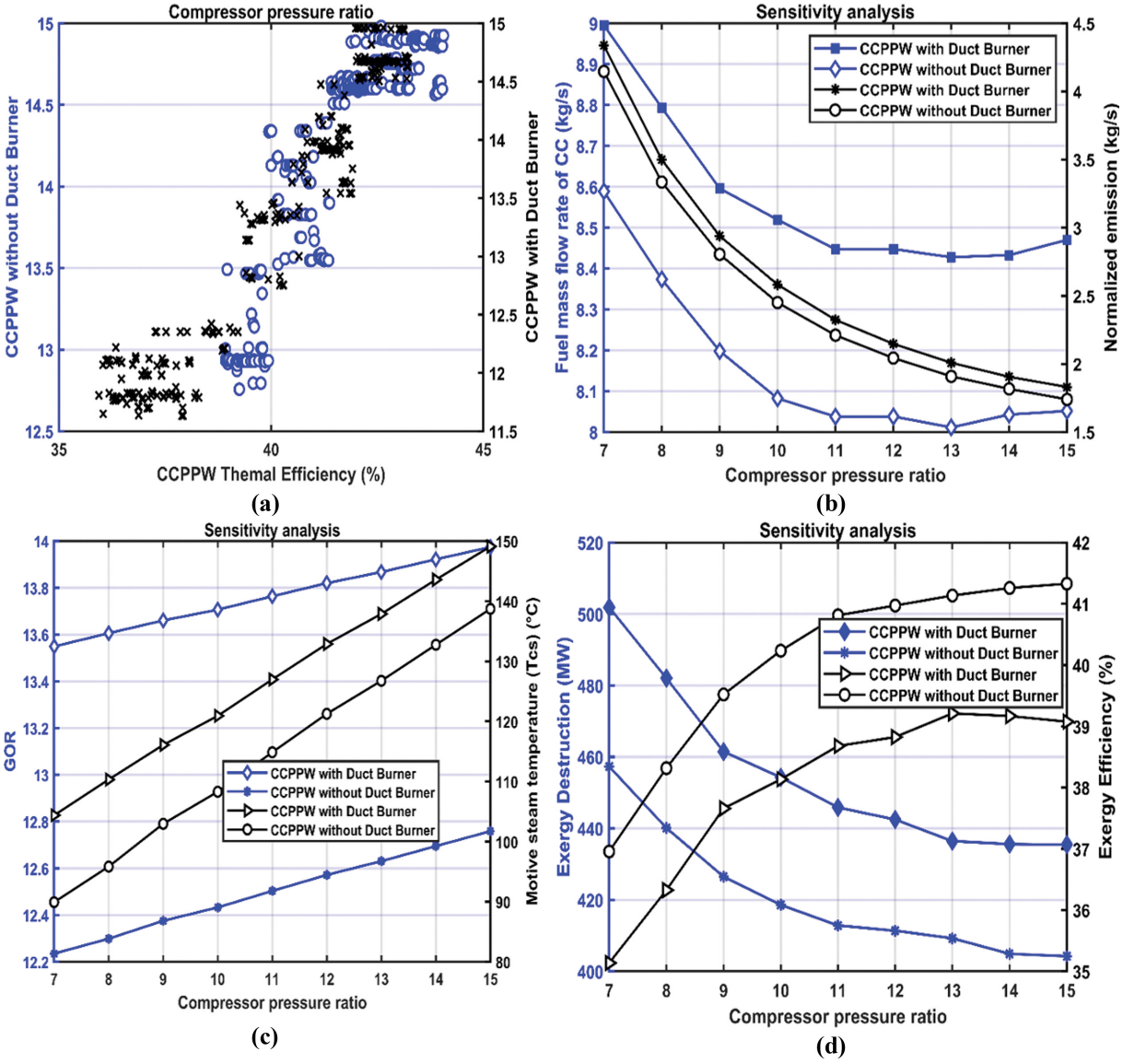

Fig. 7. (a) Effect of Compressor pressure ratio on thermal efficiency of system in Pareto optimal front, (b) Variation of fuel mass flow rate and normalized emission rate, (c) GOR and motive steam temperature, (d) exergy destruction rate and exergy efficiency.

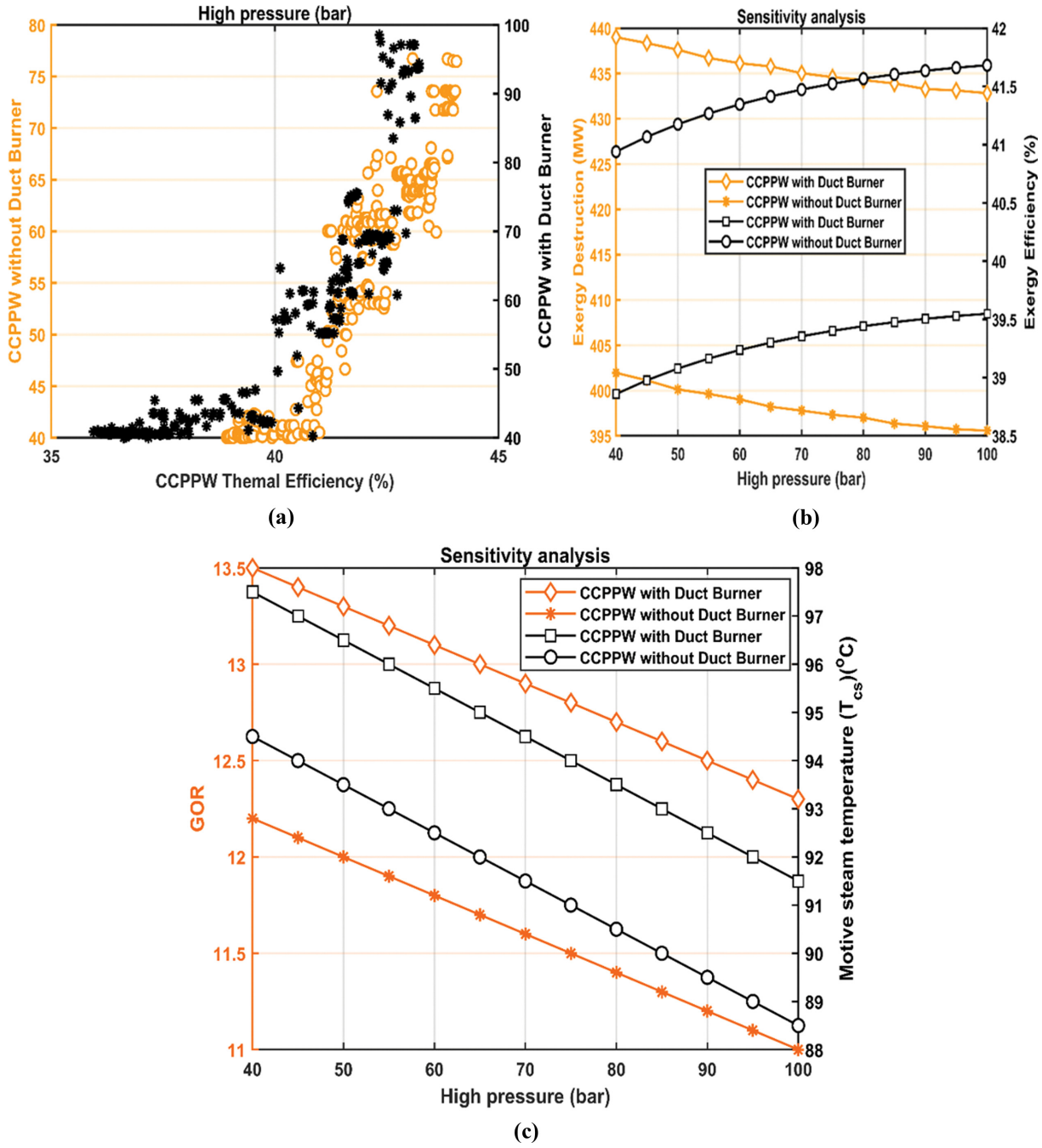

Fig. 8. (a) Effect of high pressure on thermal efficiency of system in Pareto optimal front, (b) Variation of exergy destruction rate and exergy efficiency and (c) GOR and motive steam temperature.

signing an efficient HRSG. High pressure is the operational parameter that affects the thermal efficiency of the system. It is clear that this parameter does not affect the gas cycle. Fig. 8 shows the effects of HP on the system performance parameters. According to Fig. 8(a), in the Pareto optimal front with the increase of this parameter, the thermal efficiency of the system increases. With increasing high pressure, more heat is received from hot gases. By increasing the heat transfer, more steam is recovered at the high-pressure level and, as a result, the production capacity of the steam cycle and the thermal efficiency of the combined system increase. According to Fig. 8(b) with increasing pressure, the exergy efficiency of the system increases, which is due to the increase in steam turbine power generation. Moreover, the temperature of the combustion products decreases and as a result exergy destruction rate is reduced. In addition, increasing the high-pressure level increases the heat transfer element in this level, so in the low-pressure level, less energy is being recovered because the amount of the inlet energy from the GT cycle is constant. So, according to Fig. 8(c) with increasing high-pressure, the temperature of the motive steam of the first effect and mass flow rate of motive steam decrease. As a result, the GOR of

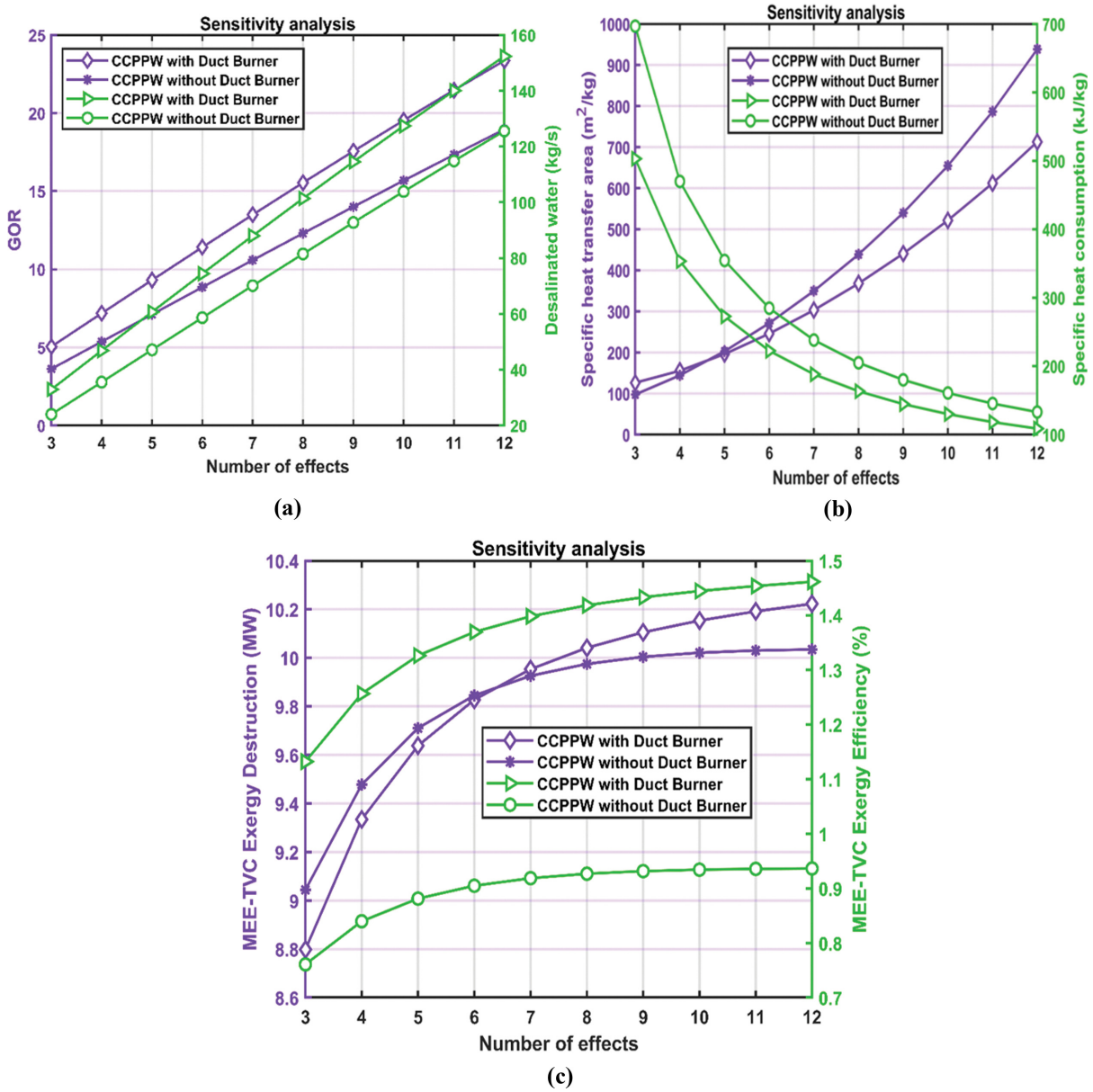

Fig. 9. (a) Impacts number effects on GOR and desalinated water, (b) specific heat consumption and specific heat transfer area and (c) exergy destruction rate and exergy efficiency.

the MEE-TVC decreases. In addition, from perspective of economic, increasing this parameter increases the annual cost by about 18%.

- **Influence of number of effects**

The number of effects is one of the most effective parameters in the performance of the MEE-TVC. According to Fig. 9(a) with increasing the number of effects and the mass flow rate of feed water to be constant, the GOR and desalinated water (freshwater production) increase, because the temperature difference between of the effects is reduced. Also, according to Fig. 9(b) as the number of effects increases and the mass flow rate and enthalpy of motive steam are constant, the specific heat consumption improves; this is due to the increase in freshwater production. So, by increasing desalinated water the specific heat transfer area increases. Fig. 9(c) shows the value of exergy efficiency and exergy destruction rate in the MEE-TVC. According to the inlet fuel exergy to be constant and with increasing the number of effects, the amount of desalinated water and the amount of the exergy production increases. Finally, with according to Eq. (37) the exergy efficiency of the MEE-TVC increases. Also, as the number of effects increases, the heat transfer steps increase and increases the exergy destruction rate. The total annual cost increases by about 3% as the number of effects increases.

- **Influence of CR of ejector**

Since the ejector has a great effect on reducing energy consumption and increasing the production of freshwater in desalination unit, its study can affect the performance of the cogeneration system. The effects of variations in the ejector compression ratio on the desalination system are shown in Fig. 10. The pressure ratio in

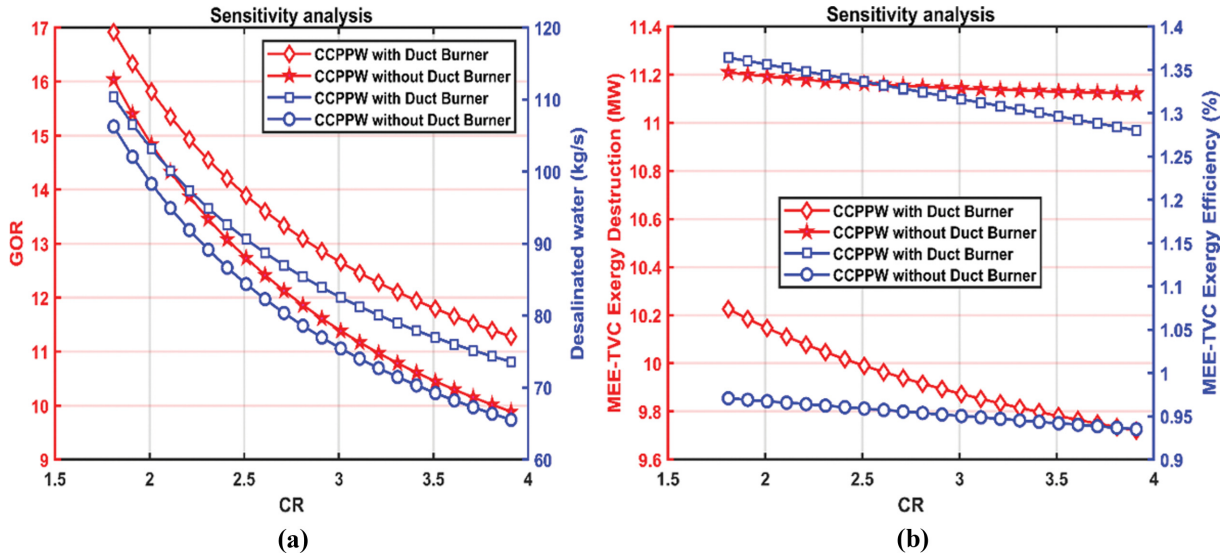

Fig. 10. (a) Effects of the CR of ejector on desalinated water and GOR and (b) MEE-TVC exergy destruction rate and exergy efficiency.

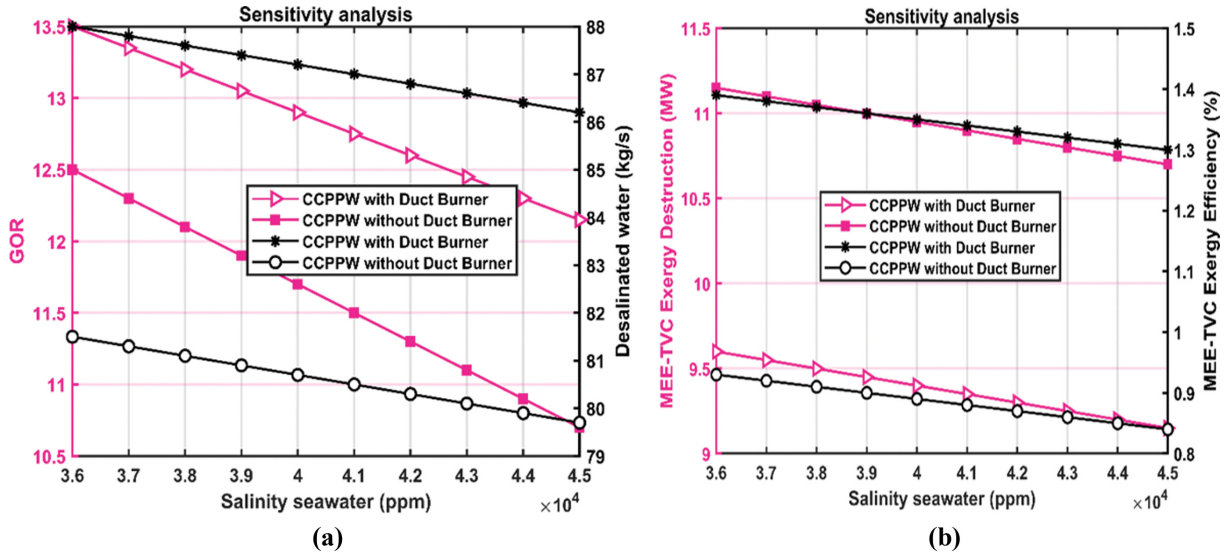

Fig. 11. (a) Effects of the seawater salinity on desalinated water and GOR, (b) MEE-TVC exergy destruction rate and exergy efficiency.

this system varies from 1.81 to 4. According to Fig. 10(a), as the pressure ratio increases, the desalinated water and GOR decreases. This is because, as the ejector compression ratio increases, more amounts of the motive steam are required to compress the secondary flow to the pressure at the ejector outlet. Therefore, for the amount of motive steam to be constant, with increasing the CR, the amount of entrained steam (steam of secondary flow) and the motive steam of the first effect decreases. Then, by reducing the steam produced (desalinated water) in the first effect, the steam produced in the other effects is also reduced. Due to the decrease in freshwater production, the exergy efficiency is also reduced. Finally, by reducing the amount of incoming steam to the effects and less heat transfer, the exergy destruction rate is reduced, which is shown in Fig. 10(b). Eventually, with increasing the compression ratio, freshwater production decreases and the TAC decreases by about 2.2%.

- **Influence of seawater salinity**

Due to the non-uniform salinity of seawater in different regions, it is necessary to evaluate this parameter on the MEE-TVC performance. Fig. 11 shows the effects of variations in the seawater salinity on the desalination system. According to Fig. 11(a), with increasing salinity of seawater, the amount of freshwater production and GOR decreases. Because with increasing salinity of seawater, the mass flow rate of seawater increases, and the steam produced decreases due to heat absorption. Also, according to Fig. 11(b), due to the decrease in freshwater production and specific heat transfer area, the exergy efficiency and exergy destruction rate are reduced. Finally, as seawater salinity increases and freshwater production decreases, the cost of water desalination decreases by about 2.5%.

- **Influence of fuel mass flow rate of DB**

Fig. 12 shows the effect of fuel mass flow rate of duct burner on

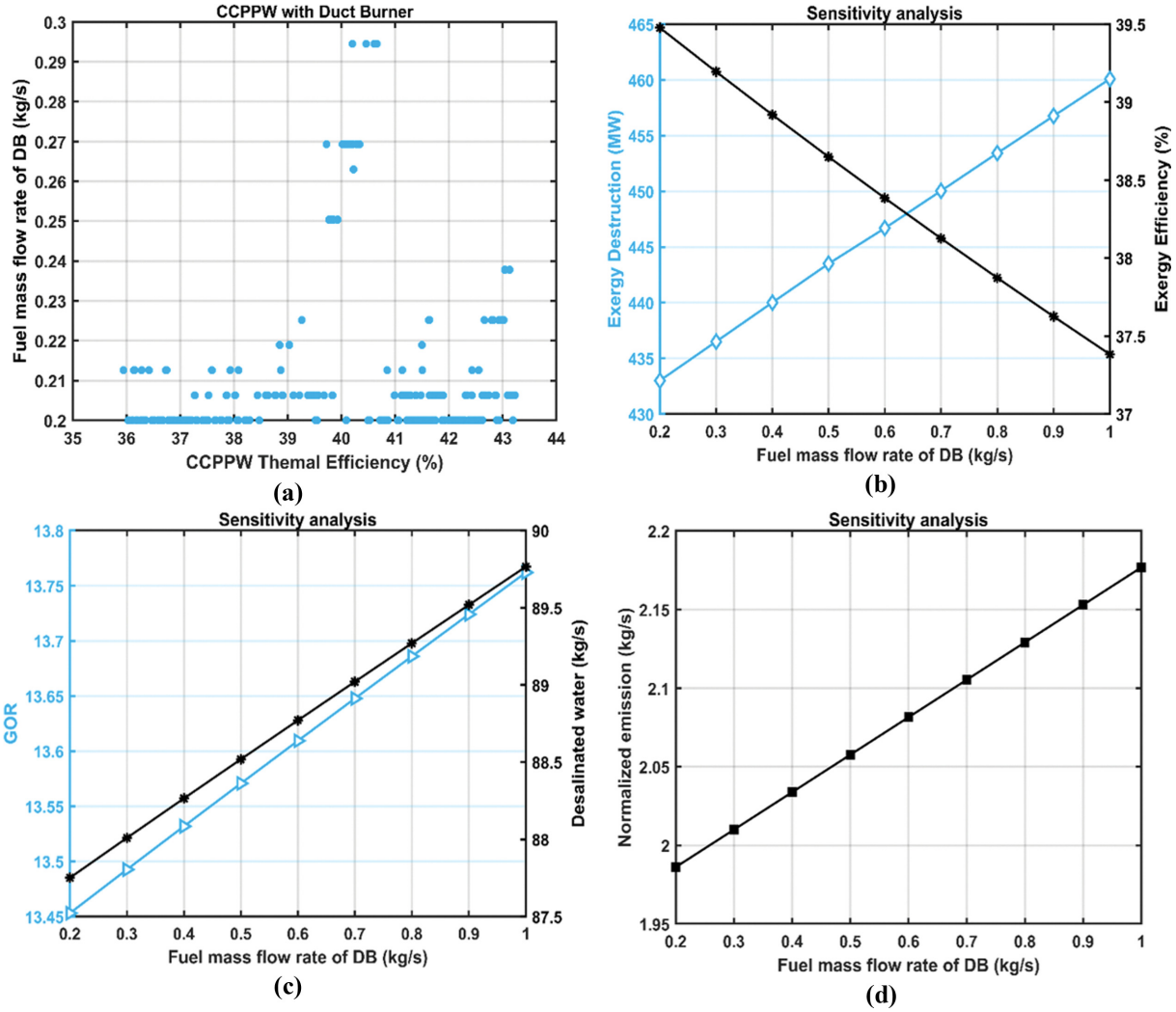

Fig. 12. (a) Effect of fuel mass flow rate of DB on thermal efficiency of system in Pareto optimal front, (b) Variation of fuel mass flow rate of DB on exergy destruction rate and exergy efficiency, (c) GOR and desalinated water, (d) normalized emission rate.

system performance. Fig. 12(a) shows the effect of fuel mass flow rate of duct burner on the thermal efficiency of the system in the Pareto optimal front, the lower bound of this parameter is selected. Because with increasing it, the cogeneration system is directed to the steam cycle and the thermal efficiency of the system decreases. Also, Fig. 12(b) shows that according to constant the net power output and increased fuel consumption in duct burner, exergy destruction rate increases and exergy efficiency decreases. Also, according to Fig. 12(c) with increasing fuel consumption, the mass flow rate and temperature of combustion products increase, and as a result, the temperature of motive steam of the desalination system increases; thus, the freshwater production and GOR increase. Finally, according to Fig. 12(d), with increasing the fuel mass flow rate of duct burner (0.2 to 1 (kg/s)), the value of pollutant emissions and TAC increases about 9.5 and 8.9%, respectively.

As a suggestion for future work: economic exergy analysis, life cycle assessment and the adding a solar section to the system. On the other hand, to achieve clean fuels such as hydrogen, the proton exchange membrane (PEM) electrolyzer can be added to the system and various analysis can be performed for it.

CONCLUSION

In the present study, thermal modeling and optimization of a cogeneration plant for simultaneous production of power and freshwater was presented. In addition, two general case studies including the mentioned system with/without duct burner were investigated. The system was optimized using multi-objective optimization technique considering 4E analysis, tacking into account the effect of energy, exergy, economic and environmental. The mentioned four parameters were summarized into the two objective functions, named thermal efficiency and total annual cost, and optimization results in each case were presented in the form of Pareto front. The optimum results revealed that the Pareto front in the case of "with duct burner" totally dominated over the results in the case of "without duct burner". The exergy analysis also showed that the combustion chamber has the highest exergy destruction. In addition, 0.67%, 3.9% and 5.9% reduction in the power pro-

duction, thermal efficiency and exergy efficiency were observed by considering the duct burner. On the other hand, 7.97% and 9.70% improvement in the freshwater production and GOR of desalination unit was obtained for the system included with duct burner.

NOMENCLATURE

A : heat transfer area [m^2]
B : brine flow rate [kg/s]
BC : Brayton cycle
bpe : boiling point elevation [°C]
$\dot{C}$: cost rate [$]
CC : combustion chamber
CR : compression ratio [-]
CRF : the capital recovery factor [-]
CO : carbon monoxide
CO_2 : carbon dioxide
Cp : specific heat [kJ/kg K]
CCPP : combined cycle power plants
CCPPW : combined cycle power plants using a desalination system
D, d : desalinated water [kg/s]
Er : expansion ratio [-]
ER : entrainment ratio [-]
ex : specific exergy [kJ/kg]
$\dot{E}x$: exergy rate [kW]
$\dot{E}x_D$: exergy destruction [kW]
F : feed water [kg/s]
GOR : gain output ratio [-]
h : enthalpy, latent heat [kJ/kg]
HRSG : heat recovery steam generator
LHV : lower heating value [kJ/kg]
LMTD : logarithmic mean temperature difference
$\dot{m}$: mass flow rate [kg/s]
M : molar weight [g/mol]
MEE-TVC : multi-effect evaporation with thermal vapor compression
N : number of particles [mole]
NEA : non equilibrium allowance [°C]
Ne : number of effects [-]
NO_x : nitrogen oxide
p : pressure [kPa, bar]
ppm : parts per million
$\dot{Q}$: heat rate [kW]
Q : specific heat consumption [kJ/kg]
Rp : pressure ratio [-]
s : specific entropy [kJ/kg·K]
T : temperature [K, °C]
TAC : total annual cost [$/year]
time : operating time of the system in one year
T_{pz} : primary zone combustion temperature
U : heat transfer coefficient [kW/m^2 K]
$\dot{W}$: power rate [kW]
X : concentration or salinity of brine [ppm]
y : system lifetime [year]
z_{eff} : The effective annual interest rate [%]
ΔP : pressure drop [kPa, bar]
ΔT : temperature difference [°C, k]

Greek Abbreviations

γ : specific heat ratio
τ : residence time [seconds]
η : efficiency [%]
φ : operation and maintenance coefficient
Φ : fuel to air equivalence ratio
ψ : atomic ratio, exergy efficiency [%]
π : dimensionless pressure
θ : dimensionless temperature
ξ : specific exergy loss for pure methane

Subscripts

a : air
ac : actual
Ac : air compressor
Aph : air per heater
B : brine
B_1 : brine of first effect
cc : combustion chamber
cs : compression steam
cond, con : condenser, condensed
cw : cooling water
ccpp : combined cycle power plant
ch : chemical
D : desalinated water
DB : duct burner
Dea-Eva : deaerator evaporator
env : environmental
cs : compression steam
es : entrained steam
f : fuel
fw : feed water
fwp : feed water pump
g : gas
Gen : power generator
GT : gas turbine
HP : high pressure
in : inlet
is : isentropic
inv : investment
LP : low pressure
ms : motive steam
Mix : mixture
n : number
Ne, ne : number effect
net : net power
o : ambient
out : outlet
p : product
pp : pinch point
ph : physical
s : steam
ST : steam turbine
tot : total

th : thermal
w : water

REFERENCES

1. M. Höök and X. Tang, *Energy Policy*, **52**, 797 (2013).
2. J. Chen, W. Xu, F. Zhang, H. Zuo, E. Jiaqiang, K. Wei and Y. Fan, *Energy Convers. Manage.*, **198**, 111927 (2019).
3. H. Zuo, G. Liu, E. Jiaqiang, W. Zuo, K. Wei, W. Hu and D. Zhong, *Sol. Energy*, **183**, 40 (2019).
4. H. Zuo, J. Tan, K. Wei, Z. Huang, D. Zhong and F. Xie, *J. Renewable Energy*, **168**, 1308 (2021).
5. J. Wang, L. Feng, X. Tang, Y. Bentley and M. Höök, *Futures*, **86**, 58 (2017).
6. A. Moran, P. J. Mago and L. M. Chamra, *Int. J. Energy Res.*, **32**(9), 808 (2008).
7. S. S. Henry, *Encyclopedia of climate and weather*, Oxford University Press, USA (1996).
8. S. A. Makkeh, A. Ahmadi, F. Esmaeilion, M. A. Ehyaei, *J. Cleaner Prod.*, **273**, 123122 (2020).
9. D. Coppitters, F. Contino, A. El-Baz, P. Breuhaus and W. De Paepe, *J. Renewable Energy*, **150**, 1089 (2020).
10. M. A. El-Nashar, *Desalination*, **134**, 7 (2001).
11. H. T. El-Dessouky and H. M. Ettouney, *Fundamentals of salt water desalination*, Elsevier (2002).
12. M. Al-Shammiri and M. Safar, *Desalination*, **126**, 45 (1999).
13. S. E. Shakib, S. R. Hosseini, M. Amidpour and C. Aghanajafi, *Desalination*, **286**, 225 (2012).
14. A. Esmaieli, P. Keshavarz, S. E. Shakib and M. Amidpour, *Int. J. Energy Res.*, **37**(12), 1440 (2013).
15. M. V. Petrovic and M. S. Mohammed, *Int. J. Therm. Sci.*, **19**(2), 447 (2015).
16. A. Mohammadi, M. Ashouri, M. H. Ahmadi, M. Bidi, M. Sadeghzadeh and T. Ming, *Energy Sci. Eng.*, **6**(5), 506 (2018).
17. P. Ahmadi, N. Enadi, H. Barzegar Avval and I. Dincer, *Int. J. Exergy.*, **11**(1), 1 (2012).
18. S. Mohtaram, H. G. Sun, J. Lin, W. Chen and Y. Sun, *Renewable Sustainable Energy Rev.*, **128**, 109898 (2020).
19. M. R. M Yazdi, F. Ommi, M. A. Ehyaeic and M. A. Rosen, *Energy Convers. Manage.*, **216**, 112944 (2020).
20. I. S. Al-Mutaz and I. Wazeer, *Desalination*, **351**, 9 (2014).
21. M. Salimi and M. Amidpour, *Energy Convers. Manage.*, **138**, 299 (2017).
22. M. Salimi, H. Akbarpour Reyhani and M Amidpour, *Desalination*, **427**, 51 (2018).
23. P. Guo, T. Li, Y. Wang and J. Li, *Desalination*, **500**, 114890 (2021).
24. P. Ahmadi, S. Khanmohammadi, F. Musharavati and M. Afrand, *Appl. Therm. Eng.*, **176**, 115414 (2020).
25. A. Alzahrani, J. Orfi and Z. Alsuhaibani, *Desalin. Water Treat.*, **55**(12), 3350 (2015).
26. A. Valero, M. A. Lozano, L. Serra, G. Tsatsaronis, J. Pisa, C. Frangopoulos and M. R. von Spakovsky, *Energy*, **19**, 279 (1994).
27. M. B. Jamnani and A. Kardgar, *Energy Sci. Eng.*, **8**(10), 3561 (2020).
28. P. Ahmadi and I. Dincer, *Energy Convers. Manage.*, **52**, 2296 (2011).
29. P. Ahmadi and I. Dincer, *Int. J. Greenhouse Gas Control*, **5**, 1540 (2011).
30. H. Hajabdollahi, P. Ahmadi and I. Dincer, *Int. J. Green Energy*, **8**, 44 (2011).
31. F. N. Alasfour, M. A. Darwish and A. O. Bin Amer, *Desalination*, **174**, 39 (2005).
32. M. Kim, D. Kim, I. J. Esfahani, S. Lee, M. Kim and C. Yoo, *Korean J. Chem. Eng.*, **34**(1), 6 (2017).
33. M. Moghimi, M. Emadi, P. Ahmadi and H. Moghadasi, *Exp. Therm. Fluid Sci.*, **141**, 515 (2018).
34. M. Ameri, P. Ahmadi and S. Khanmohammadi, *Int. J. Energy Res.*, **32**, 175 (2008).
35. M. A. Javadi, S. Hoseinzadeh, M. Khalaji and R. Ghasemiasl, *Sādhanā*, **44**(5), 1 (2019).
36. A. Lazzaretto and A. Toffolo, *Energy*, **29**, 1139 (2004).
37. O. L. Gulder, *ASME J. Eng. Gas Turbines Power*, **108**, 376 (1986).
38. N. K. Rizk and H. C. Mongia, *ASME J. Eng. Gas Turbines Power*, **115**, 612 (1993).
39. M. M. Ashour, *Desalination*, **152**(1), 191 (2003).
40. World weather online, [Online]. Available: https://www.worldweatheronline.com/. [Accessed: 05-Apr-2021].
41. Sea temperature, [Online]. Available: https://seatemperature.info/. [Accessed: 05-Apr-2021].
42. IRIMO, I.R.OF IRAN Meteorological Organization archives, [Online]. Available: http://irimo.ir/eng/index.php. [Accessed: 18-Jan-2019].
43. A. A. Bidokhti and M. Ezam, *Ocean Sci.*, **5**(1), 1 (2009).
44. M. Esrafilian and R. Ahmadi, *Desalination*, **454**, 20 (2019).
45. Z. T. Lian, K. J. Chua and S. K. Chou, *Appl. Energy*, **87**, 84 (2010).

APPENDIX A

A1. The mass and energy balance for the MEE-TVC system is presented in Table A1 [20,22,24].

APPENDIX B

The investment cost function of each type of equipment is given in Table B1. Also, some parameters related to economic analysis and operating conditions of the system are given in Table B2.

Table A1. The mass and energy balance for the MEE-TVC system [20,23,24]

Type	First effect	2 to last effect
Brine, B	$B_1=F_1-D_1$	$B_z=F_z+B_{z-1}-D_z$ z=2, 3, …, Ne
Salt concentration	$X_{B1}=\frac{F_1}{(F_1-D_1)}X_{fw}$	$X_{B,z}=\frac{X_{fw}F_z+X_{B,z-1}B_{z-1}}{B_z}$ z=2, 3, …, Ne
Distilled, D	$D_1=\frac{(D_{ms}+D_{es})h_{Dcs}-F_1C_p(T_1-T_{fw})}{H_{B1}}$	$D_z=\frac{(D_{z-1}h_{z-1}+d_{z-1}h_{z-1}+d^*_{z-1}h^*_{z-1})-F_zC_p(T_z-T_{fw})+B_{z-1}C_P(T_{z-1}-T_z)}{h_z}$
NEA	---------	$NEA^*_z=\frac{33(T_{con,z-1}-T_{s,z})^{0.55}}{T_{s,z}}$ z=2, 3, …, Ne
Feed, F	$F_1=\frac{F}{Ne}$	$F_i=\frac{F}{Ne}$
Condensed temperature, T	$T_{con,z}=T_{B,z}-bpe$ z=1, 2, 3, …, Ne	
Pressure, P	$P_{flow}=10^3\cdot\exp\left(\frac{-3{,}892.7}{T_{flow}+273.15-42.6776}+9.5\right)$	
Latent heat, h	$h_{flow}=2{,}589.583+0.9156\times T_{flow}-0.04834\times T^2_{flow}$	
Heat transfer area, A	$A_z=\frac{D_{s,z}h_{s,z}}{U_1(T_{con,z}-T_{B,z})}$ z=1, 2, 3, …, Ne	
Overall heat transfer coefficient, U	$U_z=\frac{1{,}939.4+1.40562T_{B,z}-0.0207525(T_{B,z})^2+0.0023186(T_{B,z})^3}{1{,}000}$ z=1, 2, 3, …, Ne	
Specific heat consumption, Q	$Q=\frac{D_{ms}h_{ms}}{D_{tot}}$	

Table B1. The investment cost function of each type of equipment

Equip	Cost function
Air compressor [26,33]	$C_{AC}=\left(\frac{39.5\dot{m}}{0.9-\eta_{is,AC}}\right)\left(\frac{P_B}{P_A}\right)\ln\left(\frac{P_B}{P_A}\right)$
Air preheater [26,33]	$C_{Aph}=2{,}290\left(\frac{\dot{m}_g(h_E-h_F)}{U(\Delta T_{LMTD})}\right)^{0.6}$
Combustion chamber [26,33]	$C_{CC}=\left(\frac{25.6\dot{m}_a}{0.995-\frac{P_D}{P_C}}\right)[1+\exp(0.018T_D-26.4)]$
Gas turbine [26,33]	$C_{GT}=\left(\frac{266.3\dot{m}_g}{0.92-\eta_{is,GT}}\right)\ln\left(\frac{P_D}{P_E}\right)[1+\exp(0.036T_D-54.4)]$
HRSG [26,33]	$C_{HRSG}=3{,}650\left(\left(\frac{Q_{hp,sup}}{(\Delta T_{LMTD})}\right)^{0.8}+\ldots\left(\frac{Q_{cph}}{(\Delta T_{LMTD})}\right)^{0.8}\right)+11{,}820\dot{m}_W+658\dot{m}_g$
Pump [33]	$C_{pump}=705.48(W^{0.71}_{pump})\left(1+\frac{0.2}{1-\eta_{is,pump}}\right)$
Desalination [44]	$C_{MEE\text{-}TVC}=3{,}018.8(D^{0.9795}_{pw})$
Steam condenser [45]	$C_{cond}=1{,}773\dot{m}_{s,HP}$
Steam turbine [32]	$C_{ST}=3{,}880.5(W^{0.7}_{ST})\left(1+\left(\frac{0.05}{1-\eta_{is,ST}}\right)^3\right)\times\left(1+5\times\exp\left(\frac{T_{in}-866}{10.42}\right)\right)$
Duct burner [30]	$C_{DB}=\eta_{DB}\dot{m}_{f,DB}LHV$
Power generator [45]	$C_{Gen}=60(W^{0.95}_{Gen})$

Table B2. Some parameters in the economic relations [18,30,33]

Parameter	Value
φ	1.06
z_{eff} (%)	12
Fuel cost ($/MJ)	0.004
y	20
Time	7,000×3,600
η_p (%)	0.7